SciMedCentral

Journal of Radiology & Radiation therapy

Research Article

Relative Depth-Doses of Curved and Asymmetric Ruthenium/Rhodium CIA and CIB/CIB-2 Model Applicators Used In Eye Brachytherapy

Eduardo de Paiva*

Division of Medical Physics, Institute de Radiation Protection and Dosimetry, Rio de Janeiro, Brazil

***Corresponding author**

Eduardo de Paiva, Division of Medical Physics, Institute of Radiation Protection and Dosimetry, Av. Salvador Allende 3773 Rio de Janeiro, Brazil; Tel: +55 21 2173-2847; Email: edup2112@gmail.com

Submitted: 16 March 2020

Accepted: 04 July 2020

Published: 05 July 2020

ISSN: 2333-7095

Keywords

- Asymmetric ^{106}Ru/^{106}Rh applicators; Beta point dose function; Relative depth-dose calculation

Abstract

The asymmetric CIA and CIB/CIB-2 model applicators containing the beta emitters ^{106}Ru/^{106}Rh are used in radiotherapy to treat ciliary body melanomas or melanomas close to the iris. A serious drawback in the use of these sources is the difficult determination of absorbed dose distributions around them, mainly because of the short range of the beta particles and the steep dose gradients. Furthermore, this symmetry makes the measurements and calculations even harder and may explain the very low quantity of data on them. In this work a simple numerical method was implemented to estimate the dose rates along the central and lateral axis of curved and asymmetric ^{106}Ru/^{106}Rh plaques and results have shown to differ in less than 19% compared to the only Monte Carlo simulation available.

ABBREVIATION

MC: Monte Carlo

INTRODUCTION

The spherical and asymmetric CIA and CIB/CIB-2 plaques containing the parent beta emitter ^{106}Ru in secular equilibrium with his daughter ^{106}Rh have important applications in ophthalmic brachytherapy [1]. The ^{106}Ru nuclide transforms to the ^{106}Rh nuclide by emission of a beta minus particle (half-life of 373.6 days, maximum energy of 39.4 keV, mean energy of 10 keV). The daughter ^{106}Rh also decays via beta minus emission to the ^{106}Pd (half-life of 29.8 seconds, maximum energy of 3.546 MeV, mean energy of 1.428 MeV). These applicators are concave and have a cut-out section designed to allow the treatment of ciliary body melanomas or melanomas close to the iris and this symmetry makes the measurements and calculations of dose distributions around the plaques even harder. This fact may explain the very low quantity of published data and a difficult comparison among them [2-6]. In reference [2] radiochromic film was used for the measurement of isodoses at a plane perpendicular to the plaque central axis at a 4.5 mm depth for the CIB plaque, and on the minimum and maximum central vertical planes; in reference [3] is presented a patch source model to carry out dosimetric calculations for the CCB and CIB model plaques. It is shown the isodose curves on the minimum central vertical plane of the CIB-type plaque and no results of depth-dose calculations along the central axis of the plaque were shown to allow a comparison with other data; in [4] the Monte Carlo (MC) code PENELOPE was used to study the dose distributions around the CIA and CIB/CIB-2 plaques, and a large discrepancy was found between calculations and measurements reported in [2] for the CIB model; in [5] a recent study by Hermida-López and Brualla the influence of the ^{106}Rh gamma spectrum on the MC simulation of ^{106}Ru/^{106}Rh plaques was investigated for the plaque models CCA, CCC, CCX and CIA. Finally, in another recent study by Trichter et al. [6] a partial characterization of the CIA-type plaque is made; they measured the dose rate distributions at a 3.5 mm depth from the inner surface of the plaque and once again no results of depth-dose along the plaque central axis are shown. Furthermore, the pronounced dose gradient and the short distances involved as compared with the dimensions of detectors, the complex geometry of the plaques, and a non-uniform distribution of the beta emitting material on the applicator surface may present some extra difficulties to carry out the dosimetry of these sources.

Thus, in this scenario theoretical estimations play an important role. Using MC is possible to simulate various geometries and media, and obtain results with an accuracy as good as or better than measurements, but may consume a large time of programming and computation and its implementation in a daily clinical routine may be not a simple task. On the other hand, analytical and numerical methods can also be used. They are based on the beta point-kernel dose function integration, and may give accurate results of dose distributions in a negligible time of computation as compared with MC simulation, but are applicable only for water as a medium and to a simple geometry [7,8].

In this work this last approach was used and a numerical code was developed to estimate the dose rates along the central axis of CIA and CIB/CIB-2 $^{106}Ru/^{106}Rh$ applicators (produced by Eckert & Ziegler BEBIG, GmbH, Berlin, Germany) by integration of the beta point-source dose function and the results are compared to the unique available MC calculations [4,5].

MATERIALS AND METHODS

The absorbed dose rate $J(\xi)$ around a point beta source as a function of the distance ξ is given by [9]

$$J(\xi)=\frac{B}{(\rho\nu\xi)^2}\left\{\begin{array}{l} c\left[1-\frac{\rho\nu\xi}{c}\exp\left(1-\frac{\rho\nu\xi}{c}\right)\right]+ \\ \rho\nu\xi\exp(1-\rho\nu\xi)-\rho\nu\xi\exp\left(1-\frac{\rho\nu\xi}{2}-\frac{f}{2}\right)\end{array}\right\}, \quad (1)$$

where ρ is the density of the homogeneous medium, ν is the absorption coefficient, and *c* and *f* are dimensionless parameters, with

$$\left[1-\frac{\rho\nu\xi}{c}\exp\left(1-\frac{\rho\nu\xi}{c}\right)\right]\equiv 0 \text{ for } \rho\nu\xi\geq c \text{ and } J(\xi)\equiv 0 \text{ for } \rho\nu\xi\geq f.$$

The constant *B* denotes a normalization term given by $B = 0.046\rho^2\nu^3E_\beta\alpha$, where E_β is the mean kinetic energy of the beta particles, and the constant α is expressed as a function of *c* and *f* as

$$\frac{1}{\alpha}=3c^2-(c^2-1)\exp(1)+ (3+f)\exp(1-f)-4\exp\left(1-\frac{f}{2}\right). \quad (2)$$

Equation (1) is a modification suggested by Vynckier and Wambersie [9] of the initial expression proposed by Loevinger [10] in order to match new experimental and theoretical data. In this sense, the parameter *f* was introduced and *f*/ρν represents the distance from which the beta-particle dose is required to be zero $(J(\xi) = 0)$.

Thus, the absorbed dose rate *D* at point P is obtained by integration of (1) over the plaque surface,

$$D=a_s\iint J(\xi).ds, \quad (3)$$

where a_S is the surface activity and *dS* is the area element. In the above integration we assume that the eye is formed only by water; the beta-emitting material is uniformly deposited on the concave surface of the applicator, and the presence of the metallic material used to encapsulate the radionuclide is not considered. Initially let us not consider the cut-out section, and in this case the plaque has spherical symmetry as shown in Figure 1 (top) and the dose rate *D* inside the eye can be written as

$$D=a_sR^2\iint J(\xi)\sin\phi d\phi d\theta, \quad (4)$$

where *R* is the constant radius of curvature; the angle θ is the azimuthal angle in the *xy*-plane from the *x*-axis ($0 \leq \theta \leq 2\pi$); is the polar angle from the positive *z*-axis ($0 \leq \varphi \leq \varphi_{max}$, where φ_{max} defines the size of the plaque), and the distance ξ from a point on the source to a point $P(0,0,z_0)$ located on *z*-axis is given by

$$\xi=\sqrt{R^2+Z_0^2-2RZ_0\cos\phi} \quad (5)$$

Now, the problem of the asymmetry of the actual sources

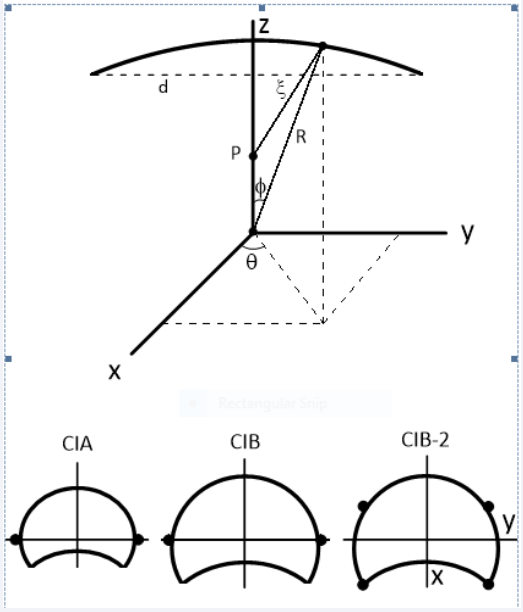

Figure 1 Geometry of the asymmetric CIA and CIB/CIB-2 ruthenium/rhodium plaques used in calculations (top). Depths increase from source surface to the origin of the system of coordinates. A *xy*-plane view of the plaques showing the position of the eyelets is also shown (bottom).

was overcome by discarding the contribution of points on the source located in the cut-out section. In this work we consider the cut-out section aligned with the *x*-axis as depicted in Figure 1 (bottom) and Figure 2, which means that we do not take into consideration the points in the *xy*-plane on the right of the curves (see the dashed lines in Figure 2):

$$y=\pm\sqrt{r_0^2-(x-x_o)^2}, \quad (6)$$

with r_0 = 0.70 cm and x_0 = 0.80 cm for the CIA plaque, and r_0 = 1.18 cm and x_0 = 1.36 cm for the CIB/CIB-2 plaque.

The double integration outlined above was implemented by means of a Fortran code based on the trapezoidal rule and for the sake of comparison results are compared to available data obtained by MC simulations [4,5].

RESULTS AND DISCUSSION

The Fortran code was used to the numerical integration of the beta-point dose function (1) to obtain the relative absorbed dose rates along the central axis of the CIA (*R* = 12 mm, active diameter *d* = 13 mm) and CIB/CIB-2 (*R* = 12 mm, active diameter *d* = 17.8 mm) concave and asymmetric ophthalmic applicators containing $^{106}Ru/^{106}Rh$. The CIB and CIB-2 plaques differ only in the number and position of eyelets used to suture the plaques to the sclera, 2 for CIB and 4 for CIB-2 (see Figure. 1, bottom), and for this reason they present the same dose distributions. In Equations. (1) to (4) the absorbing medium is water; the coefficient ν is 3.57 cm^2/g; E_β is 1.43 MeV; the parameters *c* and *f* are respectively 0.88 and 5.07, and let us consider that the surface activity a_S is 10 MBq/cm^2 for both applicators.

In Figure 3 the absorbed dose rates in water are shown for

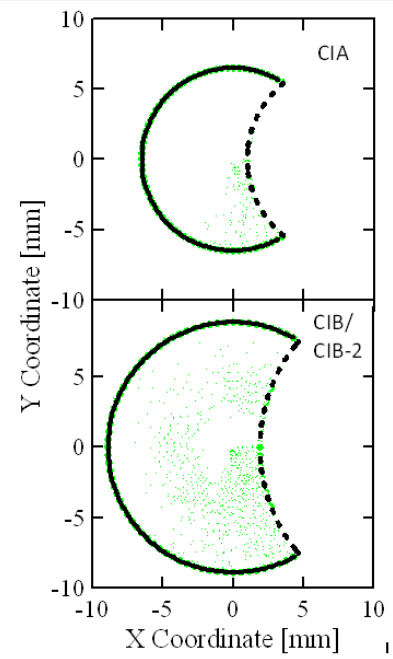

Figure 2 A *xy*-plane view of the ruthenium/rhodium plaques showing the cut-out section aligned with the *x*-axis. Top: CIA plaque, with active diameter = 13 mm and radius of curvature = 12 mm. Bottom: CIB or CIB-2 plaque, with active diameter = 17.8 mm and radius of curvature = 12 mm.

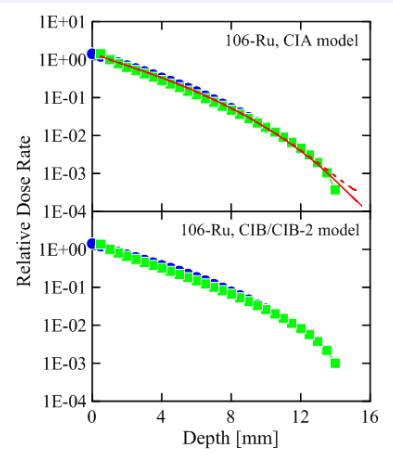

Figure 3 Relative dose rates as a function of the depth along the central axis of the CIA (top) and CIB/CIB-2 (bottom) model plaques. Squares, this work; circles, MC simulation [4]; solid line (only ^{106}Rh beta spectrum) and dashed line (gamma plus ^{106}Rh beta spectrum), MC simulations [5].

the asymmetric ^{106}Ru/^{106}Rh plaques for the CIA (top) and CIB/CIB-2 (bottom) models. They are plotted as a function of the depth along the *z*-axis and are normalised at 1 mm depth from the source surface and are compared to relative dose rates obtained by MC simulations [4,5] (with and without the inclusion of the ^{106}Rh gamma spectrum, although this contribution to the depth-dose curves is important only at depths out of the clinical interest [5]. A maximum disagreement about 19% was found for both plaques at 5-6 mm depth range. The observed disagreement may be assigned to the various simplifying hypotheses adopted. For example, the plaque (apart from the cut-out section) is considered spherically symmetric; the plaque is formed only by radioactive material; no encapsulation is considered, and the medium is homogeneous and constituted only of water.

We should note that the results obtained with MC codes may also present several sources of uncertainties. For example, in the cross sections data included in the code; in the choice of simulation parameters; the assumption that the radioisotope is uniformly distributed over the plaque surface; the assumption that the radioactive layer is infinitely thin; the assumption that the metal layer of the encapsulation has constant thickness, and the geometric modeling of the applicators. It should also be noted that large discrepancies can be observed when results of MC calculations are compared with experimental measurements for other ^{106}Ru/^{106}Rh ophthalmic plaques, and there may still be inconsistencies among the results of MC calculations with each other (see for example Figures. 2, 5, 6, 8, 9 and 11 of the work by Hermida-López [4]. Another point to be noticed is that the manufacturer provides the plaques with a calibration certificate that contains dose rate measurements along central axis with an uncertainty of ±20%.

Finally, in Figure 4 are shown the lateral dose rate distributions along *x*-axis and at 1, 2, 3, 4, 6 and 8 mm depths for the two plaques. Results are normalized to 1 at a point on the central *z*-axis at a 1 mm depth, and from the figure it can be clearly seen the effect of the cut-out section on dose distributions at greater positive values of *x*.

CONCLUSION

In this work we present numerical calculation results of relative dose rates along the central and lateral *x*-axis of the curved and asymmetric CIA and CIB/CIB-2 ruthenium plaques. In spite of the simplicity and limitations of the method used it was capable to reproduce the general behavior of dose rate

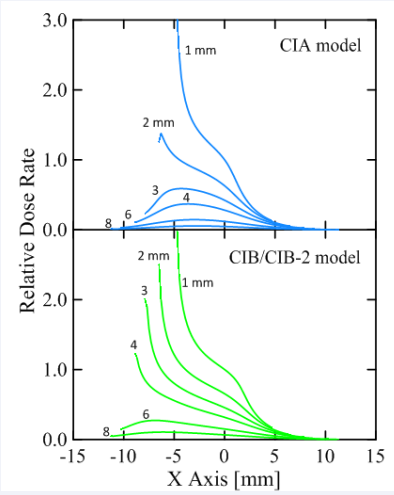

Figure 4 Relative dose rates along the lateral x-axis and at 1, 2, 3, 4, 6 and 8 mm depths for the CIA (top) and CIB/CIB-2 (bottom) model plaques.

around the applicators and it is in a moderate accordance with previously reported data obtained by means of MC simulations. Furthermore, due to the lack of data on dose distributions around these plaques, the results presented here may be useful to aid in dose planning and mainly as a guide to future experimental and theoretical studies on the CIA and CIB/CIB-2 model plaques.

REFERENCES

1. Verschueren KMS, Creutzberg CL, Schalij-Delfos NE, Ketelaars M, Klijsen FLL, Haeseker BI et al. Long-term outcomes of eye-conserving treatment with ruthenium-106 brachytherapy for choroidal melanoma. Radiother Oncol. 2010; 95: 332-338.
2. Taccini G, Cavagnetto F, Coscia G, Garelli S, Pilot A, et al. The determination of dose characteristics of ruthenium ophthalmic applicators using radiochromic film. Med Phys. 1997; 24: 2034-2037.
3. Astrahan MA. A patch source model for treatment planning of ruthenium ophthalmic applicators. Med Phys. 2003; 30: 1219-1228.
4. Hermida-López M. Calculation of dose distributions for 12 106Ru/106Rh ophthalmic applicator models with the Penelope Monte Carlo code. Med Phys. 2013; 40: 101705.
5. Hermida-López M, Brualla L. Technical note: Monte carlo study of 106Ru/106Rh ophthalmic plaques including the 106rh gamma spectrum. Med Phys. 2017; 44: 2581-2585.
6. Trichter S, Soares CG, Zaider M, Dewyngaert KJ, Dewerd LA, Kleiman NJ, et al. 15 years of 106Ru eye plaque dosimetry at memorial Sloan-Kettering cancer center and Weill Cornell medical center using radiochromic film in a solid water phantom. Biomed Phys Eng Exp. 2018; 4: 045017.
7. De Paiva E. Numerical calculation of relative dose rates from spherical 106Ru beta sources used in ophthalmic brachytherapy. Res Phys. 2015; 5: 76-77.
8. Pashazadeh A, De Paiva E, Mahmoodian N, Friebe M. Calculation of beta radiation dose of a circular y-90 skin patch: Analytical and simulation methods. Rad Phys Chem. 2020; 166: 108491.
9. Vynckier S, Wambersie A. Dosimetry of beta sources in radiotherapy. I. The beta point source dose function. Phys Med Biol. 1982; 27: 1339-1347.
10. Loevinger R. The dosimetry of beta sources in tissue. The point-source function. Radiology. 1956; 66: 55-62.

Cite this article

de Paiva E (2020) Relative Depth-Doses of Curved and Asymmetric Ruthenium/Rhodium CIA and CIB/CIB-2 Model Applicators Used In Eye Brachytherapy. J Radiol Radiat Ther 7(1): 1085.